Improvisations in phototrophy. Protein engineering and functional investigation of rhodopsin proton-pumps

Ganapathy, S.

Chapter 4

A novel chemotaxis-based directed evolution assay

Rational design for protein engineering is difficult, due to a limited structure-function understanding of proteins. Moreover, standard laboratory mutagenesis methods require several days of cloning, culturing and characterization of the corresponding mutants. Directed evolution provides a rapid and efficient alternative to improve the function of specific proteins. Here, we describe the construction of a directed evolution assay to evolve PR and GR to absorb (near-infra) red wavelengths of lights. We use chemotaxis of transformed *Escherichia coli* cells as a screening method to simultaneously select for red-shifted absorbance bands and conserved proton-pumping function of the pigments.

This chapter is under preparation for a manuscript to be submitted for publication by: S. Ganapathy, A. Razumovski, J. B. van der Steen, Q. Chen, H.J.M. de Groot, K.J. Hellingwerf and W.J. de Grip

4.1 Introduction

Protein engineering involves the optimization of the function of a protein outside its native host organism. Though straightforward in aim, it is often challenging in execution. The prediction of amino acid substitutions to modify or improve a protein's function requires detailed structural information and an understanding of the structure-function relationship. Despite this information, it is often impossible to predict *de novo* how a specific protein mutation will affect the overall function of the system. In the case of proton-pumping rhodopsins, mutations will have an impact on both their spectral properties and proton-pumping function. In addition, difficulties inherent in heterologous expression, such as poor yields and thermal stability, often require additional optimization in the novel context. These limitations in rational design have paved the way for alternative high-throughput strategies based on directed evolution.

Directed evolution is a powerful emerging technique in synthetic biology for protein engineering, which mimics natural evolution on a laboratory scale [1]. It is used to rapidly evolve and select several desired properties of a protein, without requiring any prior structural information. There are four main stages in a typical directed evolution cycle (Figure 4.1): (1) generating a library of mutant genes, (2) translation of the mutant protein in a suitable host organism, (3) high throughput screening and selection of desired phenotypes, and (4) replication of the mutant library for further characterization or the next cycle of directed evolution [2]. The screening and characterization of mutants is typically the most time consuming step in standard mutagenesis methods. In a directed evolution approach, this is primarily accomplished by coupling a specific selection criterion or advantage displayed by the host to the desired protein function.

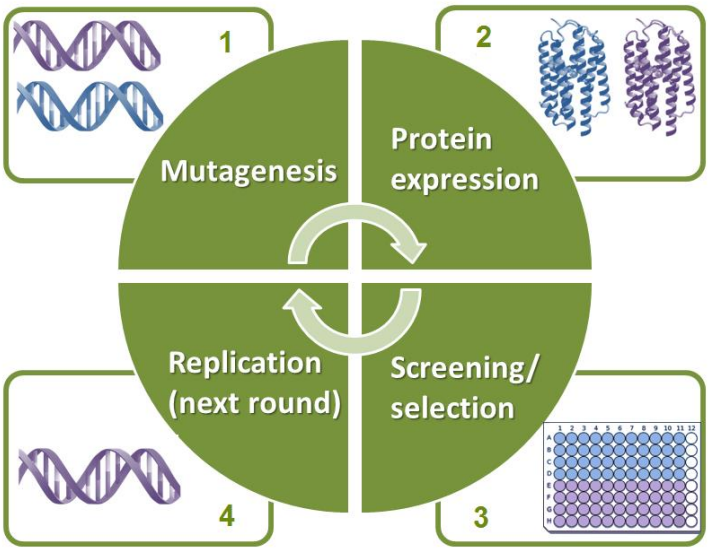

Figure 4.1 A simplified overview of the four main stages in a directed evolution cycle. All or most steps are performed in a suitable host organism.

The research aim of this chapter is the development of a directed evolution assay to rapidly evolve and select near-infra red absorbing functional variants of PR and GR. We utilized a mutagenesis plasmid [3] to generate an *in situ* library of mutations in the opsin, and further tested a number of screening strategies to simultaneously select for spectral shifts and proton-pumping activity of these mutants, using *E. coli* as a model organism for selection. Our results show that bacterial chemotaxis provides a reliable selection method when coupled with respiratory inhibition with better prospects than conventional growth or survival based assays. We thus present our design for a novel chemotaxis-based directed evolution assay for the laboratory scale evolution of rhodopsin proton-pumps.

4.2 Experimental section

The sources of special chemicals are presented in the Appendix (A.1). All chemicals are of the highest purity available.

4.2.1 Cell lines and constructs

E. coli K-12 strain MG1655 was used in this study, since it contains a deletion of the iscS gene. This deletion introduces a respiratory deficiency [4], which is explained later in this chapter. It was transformed with the plasmids pJBS1255 or pJBS1257 which encode a 6x-His tagged PR or GR opsin, respectively, driven by the inducible P_{trc} promoter, constructed as described elsewhere [5, 6]. This strain was further transformed with a mutagenesis plasmid (MUT) [3], which encodes the DNA polymerase double negative proofreading subunit dnaQ926 and error-prone repair DNA polymerase V, under control of the arabinose inducible promoter. The antibiotic resistance of the strains and plasmids used is as follows: chloramphenicol (ΔiscS), kanamycin (pJBS1255 and pJBS1257), spectinomycin (MUT).

4.2.2 Cell culturing

An overnight culture was grown in LB medium at 37 °C for 24-36 hours with appropriate antibiotic selection. The culture was diluted 1:50 times to obtain a 25 mL working culture in LB, which was grown till an OD_{600} of 0.3 and induced with 0.5 mM IPTG, 20 μM retinal and 0.1% arabinose. No retinal and arabinose were added to the controls. The cultures were further grown for 24-36 hours at 37°C and were finally spun down at 3700xg for 20 min. For the growth curve experiments, the OD_{600} of the culture was measured every hour with appropriate dilutions. The cultures were illuminated after induction with white light resulting in a photon flux of 300-400 μE.m-2.s-1.

4.2.3 Treatment with sodium azide

The cell pellet was washed once and resuspended in an equal volume of starvation buffer (SB) containing 250 mM KCl, 10 mM NaCl, 10 mM $MgSO_4$, 100 μM $CaCl_2$, 10 mM Tris-HCl at pH 7, and incubated overnight at RT with

continuous mixing. The following day, the cells were spun down at 3700xg for 20 minutes and washed once with an equal volume of SB. The cell pellet was finally resuspended in 25 mL of SB supplemented with 30 mM sodium azide (SBAz), and incubated at RT for 1 h with continuous mixing. The cells were diluted to an OD_{600} of 1.5 and directly used in the chemotaxis assay.

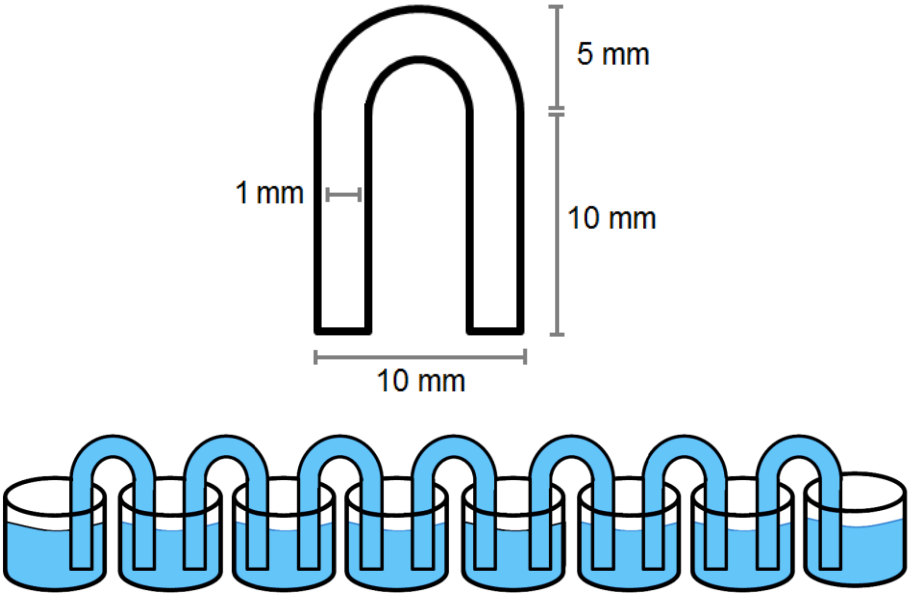

Figure 4.2 Dimensions of the U-shaped glass capillary tubes used for the chemotaxis assay and side-view of the capillaries connecting adjacent wells in a microplate.

4.2.4 Chemotaxis assay

The chemotaxis setup consists of a 96 well microplate where adjacent wells are bridged by U-shaped custom made glass capillary tubes, having an inner diameter of 1 mm, and the outer dimensions shown in figure 4.2. For initial testing and standardization of the assay, 5 wells were connected in tandem, as shown in figure 4.4. Then, 0.3 mL of the azide treated cells were loaded in well-1. Wells 2-5 were filled with 0.3 mL of 2.5, 10, 50 and 200 mM of L-serine in SBAz. The plates were sealed with a plastic cover

containing holes for the capillaries to pass through. Capillaries 1-4 were completely filled with 1, 5, 25 and 100 mM L-serine in SBAz and inserted into the wells to generate a gradient of serine, as shown in figure 4.4. The plate was illuminated for 6-10 hours from above and below with 300-800 nm white light having a photon flux of 1500 $\mu E.m^{-2}.s^{-1}$, either unfiltered or provided with 590 nm long-pass filters (OG590, Schott) resulting in a photon flux of 500 $\mu E.m^{-2}.s^{-1}$.

4.2.5 Plating of migrated colonies

After illumination, the entire content of wells 3-5 along with the previous capillary was mixed with 0.2 mL of LB medium and plated on separate LB-agar plates. The content of well-2 was diluted 10,000 times and a 0.1 mL aliquot was plated with 0.2 mL LB. The LB-agar plates were incubated at 37°C for 2-3 days, following which the number of single colonies obtained were counted as colony forming units (cfu).

4.2.6 Analysis of mutations

Individual colonies were picked using sterile toothpicks and inoculated into 5 ml LB with antibiotic selection, and grown at 37°C overnight. The following day the cultures were spun down and the total plasmid content was isolated using the QIAGEN miniprep plasmid isolation kit. The isolated plasmids were transformed into chemically competent *E. coli* XL10 to obtain a single copy of pJBS1255 or pJBS1257 per cell. The obtained colonies were cultured and used for sequencing and further characterization of the isolated mutants.

4.3 Results

4.3.1 Characterization of cell lines used and their growth rate

E. coli MG1655 Δ*isc*S, a respiratory restricted cell line, was co-transformed with two plasmids, (1) the arabinose inducible MUT which increases the error-rate during DNA replication, and (2) either pJBS1255 or pJBS1257, which encode for IPTG inducible PR or GR respectively. The controls PR_{CTRL} and GR_{CTRL} were induced with IPTG alone to generate the opsin. The wild type holo-proteins PR_{WT} and GR_{WT} were generated upon induction with IPTG and supplementation with retinal. Induction with IPTG, retinal and arabinose led to the generation of PR_{MUT} and GR_{MUT}, containing various random mutations in the opsin gene. These could be assessed by sequencing the pJBS plasmids, and could even be observed as a difference in the colour of the cell pellets (data not shown).

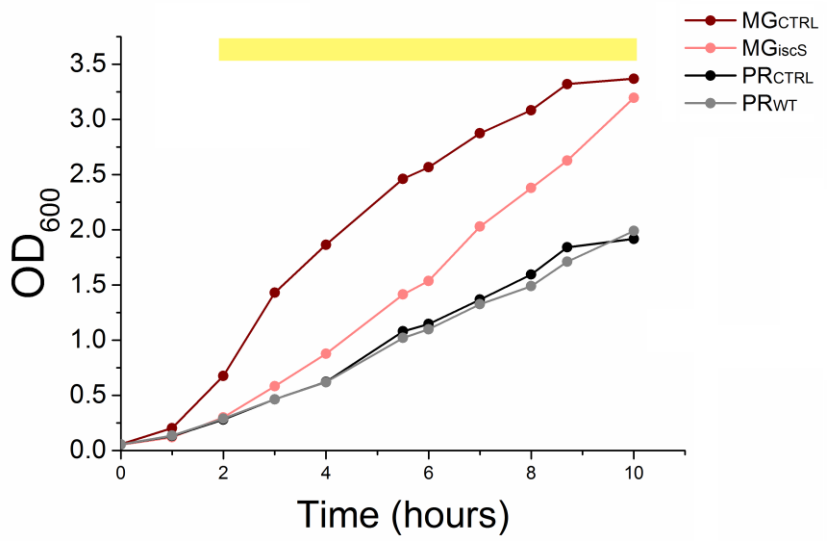

Figure 4.3 Representative growth curve of the following cell lines in LB medium at 37°C: *E. coli* MG1655 (MG_{CTRL}), *E. coli* MG1655 ΔiscS (MG_{ISCS}), *E. coli* MG1655 ΔiscS-pJBS1255-MUT induced with IPTG (PR_{CTRL}) or with IPTG and retinal A1 (PR_{WT}). The yellow bar indicates the start of induction and illumination with white light. Data is presented as an average of 3 trials; standard error is less than 1%.

We explored the possibility of using the growth of *E. coli* as a selection criterion, guided by the notion that cells can utilize the pmf generated by PR/GR for growth, especially during conditions of respiratory distress. The cells were grown in LB medium and their growth rate was assessed every hour by measuring the OD_{600} with appropriate dilutions. The doubling time of *E. coli* MG1655 Δ*isc*S was found to be around 40 minutes at 37°C, which is about twice the doubling time of WT MG1655 (Figure 4.3). In order to assess the impact of PR or GR expression upon their growth rate, the *E. coli* cultures were illuminated with white light after induction. However, no clear difference was observed between PR_{CTRL}/GR_{CTRL} and PR_{WT}/GR_{WT}, as shown in figure 4.3. We then utilized the respiratory inhibitor sodium azide, in combination with the Δ*isc*S mutation. The cells were strongly retarded in growth upon azide treatment, even at concentrations as low as 1 mM. Again, the growth rate of the controls and PR_{WT}/GR_{WT} were similar (data not shown). These data indicate that the pmf generated by PR/GR is insufficient to rescue the growth deficit prompted by respiratory inhibition. Since selection based on growth is clearly not an optimal strategy, we decided to pursue other alternatives.

We were prompted by a recent study, which showed that the pmf dependent rotation of the *E. coli* flagellar motor could be inhibited by azide treatment, but was rescued upon activation of PR [7]. The rotation of the flagellar motor enables the "swimming" of *E. coli* towards an attractant or away from a repellant, termed as bacterial chemotaxis. We thereby decided to test the possibility of using chemotaxis as a screening method in the directed evolution of PR and GR. The amino acid serine was selected as a potent chemo-attractant [8, 9].

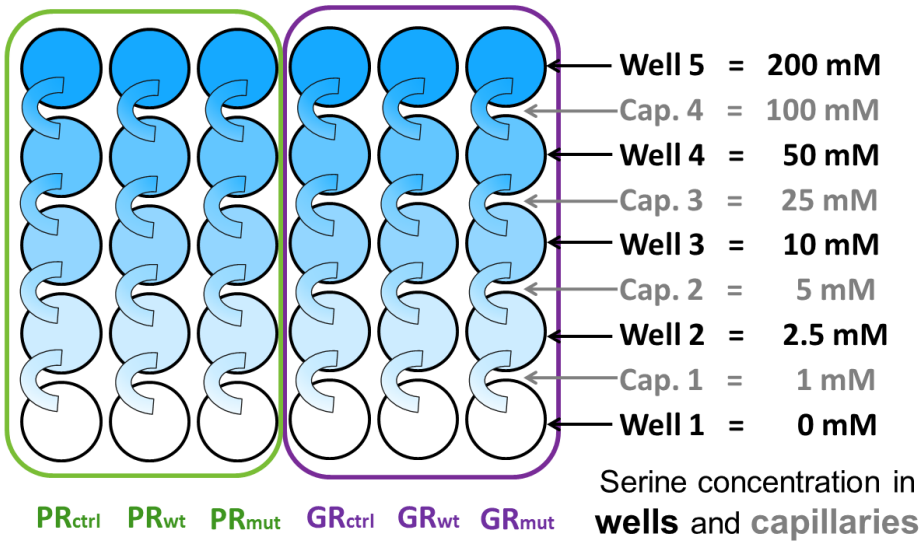

Figure 4.4 Illustration of a chemotaxis assay in which 5 adjacent wells are bridged with U-shaped capillary tubes, generating a continuous gradient of serine. The azide treated cells are loaded in well-1. *E. coli* MG1655 Δ*isc*S containing the plasmids MUT and pJBS1255 or pJBS1255, which encode for PR or GR respectively, were induced with IPTG (PR_{ctrl}, GR_{ctrl}), IPTG and retinal (PR_{wt}, GR_{wt}) or IPTG, retinal and arabinose (PR_{mut}, GR_{mut}).

4.3.2 Design of a novel chemotaxis assay

We applied a conventional 96-well microplate for the chemotaxis assay using glass capillaries to bridge adjacent wells, thereby maintaining a continuous liquid interface. These U-shaped glass capillary tubes containing an inner diameter of 1 mm were custom-made for this experiment (Figure 4.2). We first decided to test the feasibility of this assay on a small scale by bridging 5 microplate wells in tandem. This assay was optimized for the length of the capillary tubes, the serine gradient, duration of chemotaxis, duration of starvation and starting OD_{600} of cells used to achieve the maximum migration potential of PR_{WT} and GR_{WT}. The following protocol was developed under white-light illumination, and yielded consistent data providing good discrimination between control cells and cells containing active PR or GR.

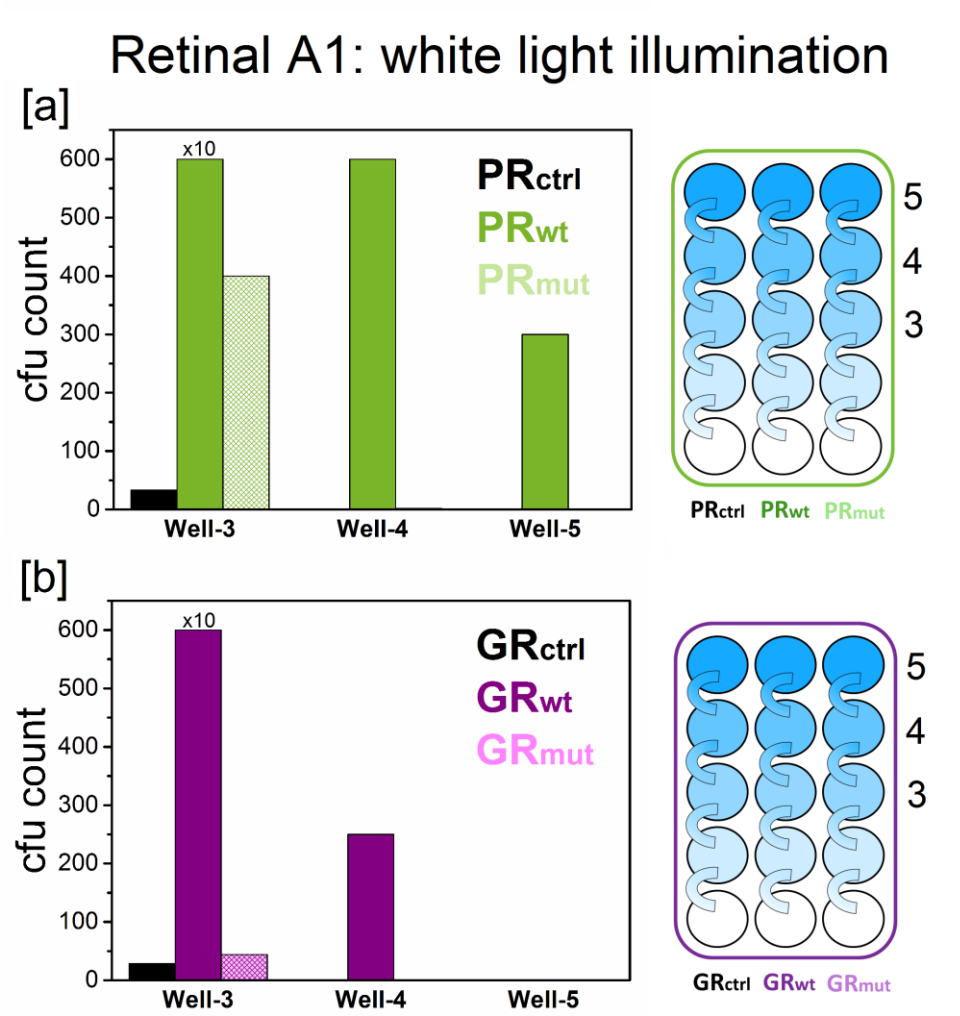

Figure 4.5 Cfu counts of migrated *E. coli* MG1655 Δ*iscS* cells expressing PR [a] or GR [b] from a representative 6 hours chemotaxis experiment under white light illumination (300-800 nm). The PR_{WT} and GR_{WT} bars for well-3 have been reduced tenfold to fit in the figure.

E. coli MG1655 Δ*iscS* cells expressing MUT and PR or GR were starved for a day in SB, followed by treatment with 30 mM azide for an hour, in order to thoroughly disrupt cellular pmf. These cells were diluted to an OD_{600} of 1.5 using a dilution curve, and then pipetted into well-1. The remaining wells and capillaries were filled with different concentrations of serine, to

generate a gradient over 5 wells, as shown in figure 4.4. The setup was illuminated for 6-10 hours and the contents of the wells were immediately plated on LB-agar. The individual colony forming units (cfu) were counted, which each represent a single migrated *E. coli* cell.

We found that PR_{WT} migrated significantly further along the serine gradient than PR_{CTRL} all the way to well-5, as seen from the cfu counts in figure 4.5. This trend was also seen to a smaller extent with GR_{WT}, which migrated till well-4. These findings were mirrored across all trials with white light illumination, indicating that the azide inhibition of chemotaxis can indeed be rescued by the pmf generated by PR and GR. However varying results were obtained for PR_{MUT} and GR_{MUT} across several trials. Overall, the mutant population was not able to migrate as far as the population with wild type. In the representative experiment shown in figure 4.5, very little migration was seen beyond well-3 for GR_{MUT} and PR_{MUT}, though their cfu counts were still higher than the controls. This is not unexpected, since the random mutagenesis process will reduce the viability of a significant part of the cell population under white-light illumination. Therefore, we decided to further test the feasibility of this assay with retinal analogs and selection with progressively red-shifted light regimes in order to confer a better selection advantage towards mutants with red-shifted rhodopsins.

4.3.3 Selection for red-shifting mutations

Retinal A2 is a promising retinal analog investigated in chapters 2 and 3 of this thesis, which generated ~40 nm bathochromic shifts in the action spectrum of both PR and GR. We thereby generated A2 pigments of PR and GR and tested them in the chemotaxis assay using illumination through 590 nm long-pass filters (590-800 nm light regime). In this case the light intensity is roughly three times lower than with the white light illumination trials, due to which the overall migration rates are lower. A representative trial is displayed in figure 4.6.

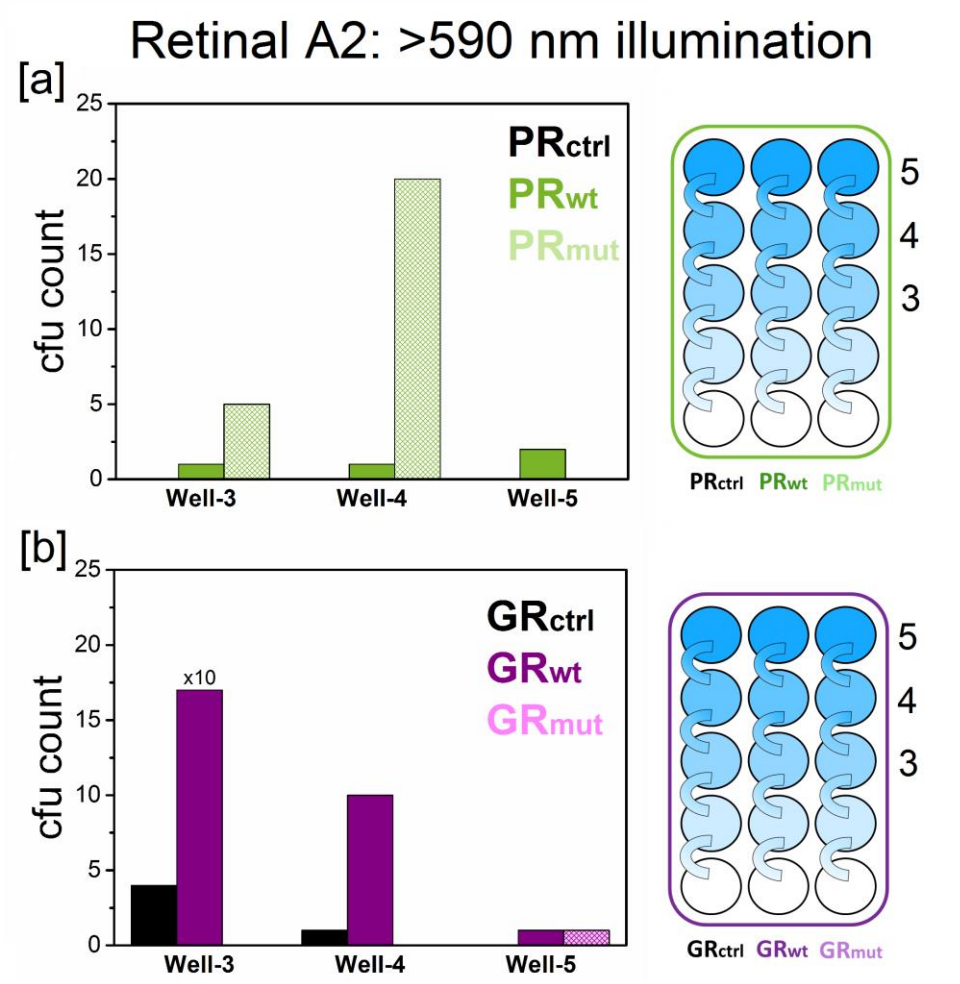

Figure 4.6 Cfu counts of migrated *E. coli* MG1655 ΔiscS cells expressing A2 pigments of PR [a] or GR [b] from a representative chemotaxis experiment, after 10 hours of 590-800 nm illumination. The GR_{WT} bar for well-3 has been reduced tenfold to fit in the figure.

Under these red-light conditions the PR_{CTRL} cells even did not reach well-3, and PR_{WT} performed less well than under white-light. However, now PR_{MUT} migrated significantly better compared to PR_{WT}. On the other hand, GR showed a trend similar to the white light illumination trials, except that some GR_{MUT} cells now managed to migrate till well-5. The individual PR_{MUT} and GR_{MUT} colonies from wells-4 and 5 were cultured and analyzed. Initial

results indicate that some of these cells indeed have generated rhodopsins with red-shifted absorbance bands (data not shown), which require further characterization.

4.4 Discussion

4.4.1 Towards a directed evolution approach

Site-directed mutagenesis is the most common method used to introduce a desired mutation at a point of interest on a gene [10]. As described earlier in this thesis, we utilized mis-match PCR to generate several site-directed mutants of PR and GR listed in the Appendix A.6. However, this approach is painstaking, requiring several days of cloning to introduce, verify, and test a specific mutation. Faster techniques such as CRISPR have now become available, which are widely used for rapid *in situ* genome editing in host organisms [11]. Site-saturation mutagenesis is another popular approach, which has the advantage of sampling all possible amino-acid substitutions at a given site [12]. This method has been employed to spectrally modulate GR by targeting residues in the retinal-binding pocket [13]. Random mutagenesis using error prone PCR has also been used to generate red and blue shifted PR mutants [14]. These different *in vitro* mutagenesis protocols have been successful in generating a handful of PR and GR mutants with variable red-shifts (5-30 nm) in absorbance maximum [13-16]. However, a common drawback in all these methods is the substantial to complete loss in proton-pumping activity of the mutants. So far the F260S mutation in GR, described in chapter 3 (9 nm red-shift) is the only one retaining full activity. Hence, a directed evolution assay, including a random mutagenesis protocol and a tight screen on both spectral properties and pump activity would be very welcome. We reasoned that the additional pmf and ATP provided by an active proton pump could be a solid basis for such a screen, and should be combined with a plasmid inducibly suppressing DNA proofreading activity.

4.4.2. Testing growth as a selection criterion

Various studies have shown that the light-induced pmf generated by proteorhodopsins can drive ATP production *in vivo* [17, 18], and it was speculated that this ATP can utilized for the growth and survival of host organisms [19, 20]. Such a growth or survival advantage can be exploited as a convenient selection criterion in designing a directed evolution setup. However, in initial experiments, little stimulatory effect of PR expression was found upon the aerobic growth of *E. coli* (Figure 4.3). This finding was mirrored by previous studies both in *E. coli* [21] and native hosts [22]. These experiments indicate that the pmf induced by PR is largely overshadowed by the endogenous pmf generated by the *E. coli* respiratory chain. PR did, however, contribute towards the growth of *E. coli* [21] or its native host *Vibrio* sp. [23] under anaerobic conditions or nutrient limitation. We thereby decided to use a strain of *E. coli* with compromised respiration, namely *E. coli* MG16555 Δ*isc*S.

Deletion of the *isc*S gene was shown to affect the formation of Fe-S clusters, which in turn impacts electron transport and pmf generation via the respiratory complexes [24, 25]. We found that *E. coli* MG16555 Δ*isc*S grew slower than its WT counterpart showing an elongated lag phase and 40 minute doubling time in agreement with what was reported previously [25]. Another study reported that *E. coli* lacking *isc* displays a pmf-dependent gentamycin resistance phenotype, which could be reversed upon PR expression [4]. We hypothesized that activation of PR or GR would also be able to reverse the growth defect induced by Δ*isc*S. However, stimulation of PR_{WT} or GR_{WT} with white light illumination did not appear to confer any significant growth advantage to the cells, indicating that the respiratory inhibition of Δ*isc*S may be insufficient for PR/GR to provide a distinct advantage. Therefore, we exerted additional respiratory pressure on the cells using the poison sodium azide, which has multiple cellular effects, including inhibition of cytochrome oxidase and of the H^+-ATPase

complex [26, 27]. Azide is a very potent poison and indeed very little growth was observed in control cells at concentrations over 1 mM (not shown). This growth inhibition persisted upon expression and activation of PR/GR. These findings indicate that the pmf generated by PR/GR is insufficient to rescue growth defects due to severe respiratory distress. Consequently, we explored other options.

4.4.3.1 Chemotaxis as a selection criterion

The rotation of the flagellar motor in *E. coli* is another important cellular process powered by pmf [28], which drives the movement of the cell towards or away from a chemical source. In the absence of a chemical gradient, *E. coli* exhibits random swimming behavior consisting of alternate "runs" and "tumbles". Upon applying a chemical gradient, the cells modulate their tumbling frequency to swim towards a chemoattractant or away from a chemorepellant [29], termed as chemotaxis. A recent study showed that the rotation of the *E. coli* flagellar motor could be inhibited by treatment with azide, but could be rescued by expression and activation of PR [7]. Based on these findings, we conceived the idea of using bacterial chemotaxis towards a chemoattractant in energy-depleted cells as a potential selection criterion. We were inspired by the pioneering work of Julius Adler to measure and quantify bacterial chemotaxis using capillary tubes [30, 31], showing that bacteria brought into contact with a capillary filled with a chemoattractant will readily migrate into the tube. We adapted this concept using U-shaped glass capillary tubes and converted a conventional 96 well microplate into a chemotaxis screening set-up. Serine was selected as a chemoattractant in our assay, since it is very potent and has been commonly employed to measure and quantify chemotaxis in *E. coli*. [8, 9]. A pre-determined step-gradient of serine was filled in the capillaries and wells, which would produce a more or less continuous gradient by diffusion. The migratory rate of healthy *E. coli* cells towards serine is reported to be between 15-20 $\mu m.s^{-1}$ [8]. Given the dimensions of

the capillaries used and the starvation of the cells, we estimated that the distance between 5 wells could be covered in 5-6 hours under high-intensity white light illumination, while requiring longer time-spans with low-intensity NIR illumination.

4.4.3.2 Potential of the developed chemotaxis assay

E. coli MG16555 Δ*iscS* transformed with MUT and PR/GR was selectively induced to generate CTRL, WT and MUT cells. All cell populations were energy depleted for a day by starvation and treatment with 30 mM azide. The cells were loaded in the chemotaxis assay and allowed to migrate under illumination through the capillaries following the serine gradient. Plating the contents of the wells at the end of the assay and counting the individual cells allowed us to determine how far and how many cells had migrated in the setup. We observed that under white light illumination, PR_{WT} cells indeed were able to reach well-5 in about 6 hours. Importantly, we found that under white light illumination, PR_{WT} and GR_{WT} migrated substantially further than their corresponding controls assayed without retinal supplementation, consistently across several trials.

The assay showed excellent discriminatory potential. Out of the about 10^9 cells in the starting cells, only several tens of control cells made it into well-3, while for PR_{WT} and GR_{WT} this number varied between 5-10 x 10^3. In fact, up to several tens of the latter cells could reach well-5. Not unexpectedly, both PR_{MUT} and GR_{MUT} showed impaired migration as compared to PR_{WT} and GR_{WT}. Induction of MUT, which suppresses proof-reading and enhances error-prone lesion bypass, would generate a diverse library of non-specific mutations [3]. In this case it is impossible to exclude the possibility of mutations in the bacterial genome, which could impair chemotactic migration, or generate non-functional mutations of the PR/GR gene. This would decrease the viability of a significant part of the cell population and should account for the lower migration seen for the mutant population,

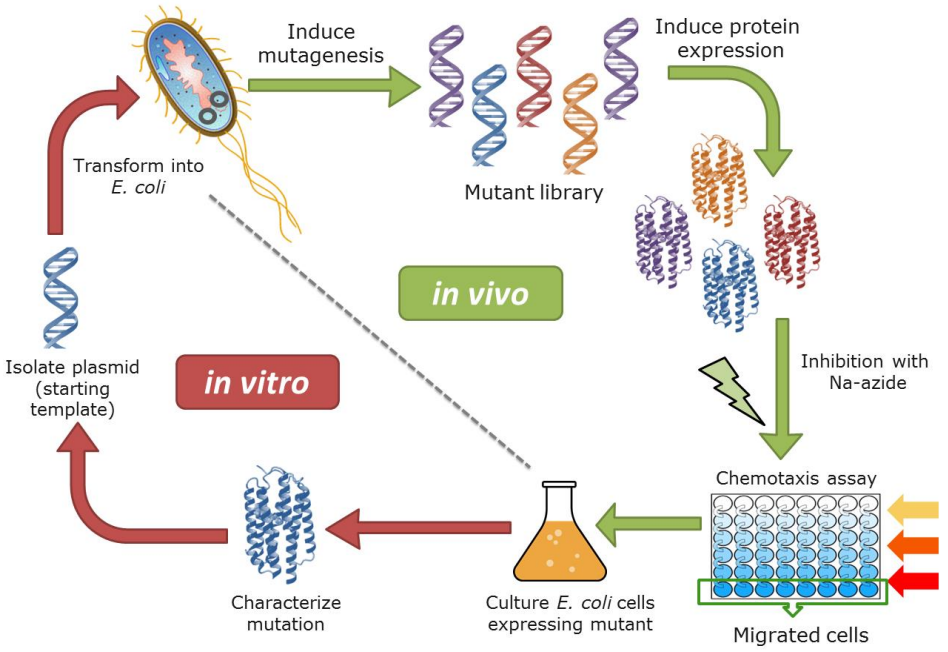

Figure 4.7 A schematic of the developed directed evolution assay using chemotaxis

Nonetheless, we were bolstered by the fact that GR_{MUT} and PR_{MUT} in particular showed better migration as compared to the corresponding controls. Hence, we proceeded to the planned assay conditions, starting with red-light illumination (>590 nm). In a first test, we additionally used the red-shifting analog A2 as a chromophore (c.f. chapters 2 and 3). In view of its absorbance spectrum, peaking at 552 nm (c.f. chapter 3), the A2 pigment of PR_{WT} migrated less well than under white light as expected. However, now the A2 pigment of GR_{WT} showed improved migration relative to PR_{WT}, most likely due to its more red-shifted action spectrum, and yielded a distribution pattern over the wells quite similar to that under white-light illumination. Most importantly, a very positive result was that A2 pigments of PR_{MUT} showed a substantial improvement in migration as compared to PR_{WT}. Preliminary characterization of these migrated cells indeed gave evidence for the presence of red-shifted action spectra.

4.4.3.3. Prospects of the chemotaxis assay

The red-light screen described above should be repeated several times to sample as many positive mutants as possible, in view of the random character of the mutagenesis process. Promising mutants will be subjected to additional screens with further red-shifted photons (> 650 nm). If sufficient intensity can be attained in the 650-800 nm range (> 1000 $\mu E.cm^{-2}.s^{-1}$), the assay will also be performed with MMAR as a ligand (c.f. chapter 3), aiming at further enhancing the NIR absorbance band and increasing the proton pumping activity.

4.5 Conclusion

In summary, we designed a novel assay, which uses bacterial chemotaxis as a selection criterion in a directed evolution scheme (Figure 4.7). This assay was aimed towards the evolution of red-shifted rhodopsin proton-pumps, which have much potential as synthetic biology tools and for various nanobiotechnological devices [32]. The developed assay shows strong discriminatory power, and in principle, can be easily modified to evolve other cellular systems dependent on illumination, energy or transport.

References

[1] Cobb, R. E., Sun, N. and Zhao, H. "Directed evolution as a powerful synthetic biology tool ", *Methods*, 2013. **60**(1): p. 81-90.

[2] Packer, M. S. and Liu, D. R. "Methods for the directed evolution of proteins ", *Nat Rev Genet*, 2015. **16**(7): p. 379-394.

[3] Esvelt, K. M., Carlson, J. C. and Liu, D. R. "A system for the continuous directed evolution of biomolecules ", *Nature*, 2011. **472**(7344): p. 499-503.

[4] Ezraty, B., Vergnes, A., Banzhaf, M., Duverger, Y., Huguenot, A., Brochado, A. R., Su, S. Y., Espinosa, L., Loiseau, L., Py, B., Typas, A. and Barras, F. "Fe-S cluster biosynthesis controls uptake of aminoglycosides in a ROS-less death pathway ", *Science*, 2013. **340**(6140): p. 1583-7.

[5] Chen, Q., van der Steen, J. B., Dekker, H. L., Ganapathy, S., de Grip, W. J. and Hellingwerf, K. J. "Expression of holo-proteorhodopsin in Synechocystis sp. PCC 6803 ", *Metab Eng*, 2016. **35**: p. 83-94.

[6] Chen, Q., Arents, J., Ganapathy, S., de Grip, W. J. and Hellingwerf, K. J. "Functional expression of Gloeobacter rhodopsin in *Synechocystis* sp. PCC6803 ", *Photochem Photobiol*, 2017. **93**(3): p. 772-781.

[7] Walter, J. M., Greenfield, D., Bustamante, C. and Liphardt, J. "Light-powering *Escherichia coli* with proteorhodopsin ", *Proc Natl Acad Sci U S A*, 2007. **104**(7): p. 2408-12.

[8] Vuppula, R. R., Tirumkudulu, M. S. and Venkatesh, K. V. "Chemotaxis of *Escherichia coli* to L-serine ", *Phys Biol*, 2010. **7**(2): p. 026007.

[9] Mesibov, R. and Adler, J. "Chemotaxis toward amino acids in *Escherichia coli* ", *J Bacteriol*, 1972. **112**(1): p. 315-26.

[10] Ling, M. M. and Robinson, B. H. "Approaches to DNA mutagenesis: an overview ", *Analytical biochemistry*, 1997. **254**(2): p. 157-78.

[11] Hsu, P. D., Lander, E. S. and Zhang, F. "Development and Applications of CRISPR-Cas9 for Genome Engineering ", *Cell*, 2014. **157**(6): p. 1262-1278.

[12] Reetz, M. T. and Carballeira, J. D. "Iterative saturation mutagenesis (ISM) for rapid directed evolution of functional enzymes ".

[13] Engqvist, M. K., McIsaac, R. S., Dollinger, P., Flytzanis, N. C., Abrams, M., Schor, S. and Arnold, F. H. "Directed evolution of *Gloeobacter violaceus* rhodopsin spectral properties ", *J Mol Biol*, 2015. **427**(1): p. 205-20.

[14] Kim, S. Y., Waschuk, S. A., Brown, L. S. and Jung, K. H. "Screening and characterization of proteorhodopsin color-tuning mutations in *Escherichia coli* with endogenous retinal synthesis ", *Biochim Biophys Acta*, 2008. **1777**(6): p. 504-13.

[15] Maiti, T. K., Yamada, K., Inoue, K. and Kandori, H. "L105K Mutant of Proteorhodopsin ", *Biochemistry*, 2012. **51**(15): p. 3198-3204.

[16] Yamada, K., Kawanabe, A. and Kandori, H. "Importance of alanine at position 178 in proteorhodopsin for absorption of prevalent ambient light in the marine environment ", *Biochemistry*, 2010. **49**(11): p. 2416-23.

[17] Martinez, A., Bradley, A. S., Waldbauer, J. R., Summons, R. E. and DeLong, E. F. "Proteorhodopsin photosystem gene expression enables photophosphorylation in a heterologous host ", *Proc Natl Acad Sci U S A*, 2007. **104**(13): p. 5590-5.

[18] Lee, K. A. and Jung, K.-H. "ATP Regeneration System Using *E. coli* ATP Synthase and *Gloeobacter* Rhodopsin and Its Stability ", *J Nanosci Nanotechnol*, 2011. **11**(5): p. 4261-4264.

[19] Beja, O., Spudich, E. N., Spudich, J. L., Leclerc, M. and DeLong, E. F. "Proteorhodopsin phototrophy in the ocean ", *Nature*, 2001. **411**: p. 786-789.

[20] Gómez-Consarnau, L., González, J. M., Coll-Lladó, M., Gourdon, P., Pascher, T., Neutze, R., Pedrós-Alió, C. and Pinhassi, J. "Light stimulates growth of proteorhodopsin-containing marine Flavobacteria ", *Nature*, 2007. **445**(7124): p. 210-213.

[21] Wang, Y., Li, Y., Xu, T., Shi, Z. and Wu, Q. "Experimental evidence for growth advantage and metabolic shift stimulated by photophosphorylation of proteorhodopsin expressed in *Escherichia coli* at anaerobic condition ", *Biotechnol Bioeng*, 2015. **112**(5): p. 947-56.

[22] Walter, J. M., Greenfield, D. and Liphardt, J. "Potential of light-harvesting proton pumps for bioenergy applications ", *Curr Opin Biotechnol*, 2010. **21**(3): p. 265-70.

[23] Gómez-Consarnau, L., Akram, N., Lindell, K., Pedersen, A., Neutze, R., Milton, D. L., González, J. M. and Pinhassi, J. "Proteorhodopsin phototrophy promotes survival of marine bacteria during starvation *", PLoS Biol*, 2010. **8**(4): p. e1000358.

[24] Schwartz, C. J., Djaman, O., Imlay, J. A. and Kiley, P. J. "The cysteine desulfurase, IscS, has a major role in in vivo Fe-S cluster formation in *Escherichia coli", Proc Natl Acad Sci U S A*, 2000. **97**(16): p. 9009-14.

[25] Lauhon, C. T. and Kambampati, R. "The iscS gene in Escherichia coli is required for the biosynthesis of 4-thiouridine, thiamin, and NAD *", J Biol Chem*, 2000. **275**(26): p. 20096-103.

[26] Noumi, T., Maeda, M. and Futai, M. "Mode of inhibition of sodium azide on H+-ATPase of Escherichia coli *", FEBS Letters*, 1987. **213**(2): p. 381-384.

[27] Lichstein, H. C. and Soule, M. H. "Studies of the effect of sodium azide on microbic growth and respiration: II. The action of sodium azide on bacterial catalase *", J Bacteriol*, 1944. **47**(3): p. 231-8.

[28] Gabel, C. V. and Berg, H. C. "The speed of the flagellar rotary motor of Escherichia coli varies linearly with protonmotive force *", Proc Natl Acad Sci U S A*, 2003. **100**(15): p. 8748-51.

[29] Vladimirov, N. and Sourjik, V. "Chemotaxis: how bacteria use memory *", Biological chemistry*, 2009. **390**(11): p. 1097-104.

[30] Adler, J. "Chemoreceptors in Bacteria *", Science*, 1969. **166**: p. 1588-1597.

[31] Adler, J. "Chemotaxis in Bacteria *", Annu. Rev. Biochem.*, 1975. **44**: p. 341-356.

[32] Wagner, N. L., Greco, J. A., Ranaghan, M. J. and Birge, R. R. "Directed evolution of bacteriorhodopsin for applications in bioelectronics *", J R Soc Interface*, 2013. **10**(84).